Numerical investigation of shock wave – dense particles cloud interaction

Pavel S. Utkin
Moscow Institute of Physics and Technology
Dolgoprudny, Moscow region, Russia
Institute for Computer Aided Design of the Russian Academy of Sciences
Moscow, Russia

1 Introduction

A lot of both experimental and theoretical investigations of two-phase flows with shock waves (SW) deal with dusty gas but not much works address to the dense two-phase flows. The models based on the kinetic theory for granular flows [1 – 3] and Baer-Nunziato (BN) equations [4, 5] as well as some hybrid models [6] are among the number of popular approaches which make it possible to describe the dense high-speed two-phase media motion in the Euler-Euler statement. Moreover the up to date problem is the construction of numerical procedures efficient for the calculation of two-phase flows with wide range of possible regimes – from dilute with low dispersed phase volume fraction to the dense with the dispersed phase volume fraction close to the packing limit. Such low-dissipation numerical method for the solution of Gidaspow model equations was proposed recently in [2].
A canonical problem that can be used to study modeling issues related to the dense high speed multiphase flows is a SW impacting a planar particle cloud [7]. The problem in [7] was solved numerically in two-dimensional statement and the obtained results were compared with predictions made by the specially derived one-dimensional phase-averaged equations.
The aim of the work is the numerical investigation of the SW – dense particles cloud interaction with the use of Godunov solver for BN equations [8] and the comparison of the obtained results with the experimental data [9].

2 Mathematical model

Mathematical model is based on the reduced BN system of equations for the two-phase compressible media problems [4] originally formulated for the investigation of deflagration-to-detonation transition in heterogeneous explosives:

$$\mathbf{u}_t + \mathbf{f}_x(\mathbf{u}) = \mathbf{h}(\mathbf{u})\bar{\alpha}_x + \mathbf{s}, \qquad (1)$$

Here,

$$\mathbf{u} = \begin{bmatrix} \bar{\alpha} \\ \bar{\alpha}\bar{\rho} \\ \bar{\alpha}\bar{\rho}\bar{v} \\ \bar{\alpha}\bar{\rho}\bar{E} \\ \alpha\rho \\ \alpha\rho v \\ \alpha\rho E \end{bmatrix},\ \mathbf{f} = \begin{bmatrix} 0 \\ \bar{\alpha}\bar{\rho}\bar{v} \\ \bar{\alpha}(\bar{\rho}\bar{v}^2 + \bar{p}) \\ \bar{\alpha}\bar{v}(\bar{\rho}\bar{E} + \bar{p}) \\ \alpha\rho v \\ \alpha(\rho v^2 + p) \\ \alpha v(\rho E + p) \end{bmatrix},\ \mathbf{h} = \begin{bmatrix} -\bar{v} \\ 0 \\ p \\ p\bar{v} \\ 0 \\ -p \\ -p\bar{v} \end{bmatrix},\ \mathbf{s} = \begin{bmatrix} 0 \\ 0 \\ -f \\ -f \cdot \bar{v} \\ 0 \\ f \\ f \cdot \bar{v} \end{bmatrix},$$

where

$$\bar{\alpha} + \alpha = 1,\ \bar{E} = \frac{\bar{v}^2}{2} + \frac{\bar{p} + \bar{\gamma}\bar{P}_0}{\bar{\rho}\left(\bar{\gamma} - 1\right)},\ E = \frac{v^2}{2} + \frac{p}{\rho\left(\gamma - 1\right)}.$$

The system comprises the mass, momentum and energy conservation equations for the gas and dispersed phases as well as the compaction equation for the dispersed phase volume fraction. The notations are standard. The bar superscript is used to indicate the dispersed phase quantities. The dispersed phase is described with the use of stiffened gas equation of state with the constants $\bar{\gamma}$ and $\bar{P}_0$. The non-differential right-hand side vector **s** takes into account the inter-phase friction force:

$$f = -\frac{3}{4} C_d \frac{\rho}{d} \bar{\alpha}\left(v - \bar{v}\right)\left|v - \bar{v}\right|, \tag{2}$$

where C_d is drag coefficient and d is the particles diameter. The right-hand side term in the compaction equation is omitted because the problem in consideration (see below) is characterized by the dispersed phase volume fraction close to the packing limit [10].
The properties of homogeneous system (1) with **s** = **0** are well known. It is hyperbolic under the following conditions are met:

$$\alpha \neq 0,\ \bar{\alpha} \neq 0,\ \left(v - \bar{v}\right)^2 \neq c^2, \tag{3}$$

and has no conservative form. The fact of BN system of equations hyperbolicity provides the opportunity to construct Godunov-type solvers for BN equations numerical integration.

3 Numerical method

The computational algorithm is based on the physical processes splitting technique [11] when on the time step at first the homogeneous BN systems of equations (1) with **s** = **0** is integrated and then the inter-phase interaction terms are taken into account. The homogeneous BN systems of equations is solved numerically using Godunov approach proposed in [8] which has a typical for hyperbolic system of equations form of notation (n and j are time and spatial indexes correspondingly):

$$\mathbf{U}_j^{n+1} = \mathbf{U}_j^n - \frac{\Delta t}{\Delta x}\left[\mathbf{F}_L\left(\mathbf{U}_j^n, \mathbf{U}_{j+1}^n\right) - \mathbf{F}_R\left(\mathbf{U}_{j-1}^n, \mathbf{U}_j^n\right)\right],$$

except the fact that:

$$\mathbf{F}_L\left(\mathbf{U}_{j-1}^n, \mathbf{U}_j^n\right) = \begin{cases} \mathbf{f}\left(\mathbf{u}^*\left[\mathbf{U}_{j-1}^n, \mathbf{U}_j^n\right]\right) - \mathbf{H}\left(\mathbf{U}_{j-1}^n, \mathbf{U}_j^n\right), & \text{if } \bar{v}_{c,j-1/2}^n < 0, \\ \mathbf{f}\left(\mathbf{u}^*\left[\mathbf{U}_{j-1}^n, \mathbf{U}_j^n\right]\right), & \text{if } \bar{v}_{c,j-1/2}^n > 0, \end{cases} \tag{4}$$

$$\mathbf{F}_R\left(\mathbf{U}_{j-1}^n,\mathbf{U}_j^n\right)=\begin{cases}\mathbf{f}\left(\mathbf{u}^*\left[\mathbf{U}_{j-1}^n,\mathbf{U}_j^n\right]\right), & \text{if } \overline{v}_{c,j-1/2}^n<0,\\ \mathbf{f}\left(\mathbf{u}^*\left[\mathbf{U}_{j-1}^n,\mathbf{U}_j^n\right]\right)+\mathbf{H}\left(\mathbf{U}_{j-1}^n,\mathbf{U}_j^n\right), & \text{if } \overline{v}_{c,j-1/2}^n>0.\end{cases} \tag{5}$$

Here $\mathbf{u}^*[.,.]$ is the solution of the Riemann problem for BN equations for the correspondent left and right states, $\overline{v}_{c,j+1/2}^n$ is solid contact velocity. The central part of the Riemann problem solution is the usage of special analogies of Rankine-Hugoniot relations on the solid contact [8, 12]. The exact solution of the Riemann problem also provides the exact integration of non-conservative differential right-hand side terms connected with gradients of dispersed phase volume fraction that appears as the non-conservative part of the numerical flux in (4), (5):

$$\mathbf{H}\left(\mathbf{U}_{j-1}^n,\mathbf{U}_j^n\right)=\begin{bmatrix}-\overline{v}_{c,j-1/2}^n\left(\overline{\alpha}_j^n-\overline{\alpha}_{j-1}^n\right)\\ 0\\ \overline{p}_{2,j-1/2}^n\overline{\alpha}_j^n-\overline{p}_{1,j-1/2}^n\overline{\alpha}_{j-1}^n\\ \overline{v}_{c,j-1/2}^n\left(\overline{p}_{2,j-1/2}^n\overline{\alpha}_j^n-\overline{p}_{1,j-1/2}^n\overline{\alpha}_{j-1}^n\right)\\ 0\\ -\overline{p}_{2,j-1/2}^n\overline{\alpha}_j^n+\overline{p}_{1,j-1/2}^n\overline{\alpha}_{j-1}^n\\ -\overline{v}_{c,j-1/2}^n\left(\overline{p}_{2,j-1/2}^n\overline{\alpha}_j^n-\overline{p}_{1,j-1/2}^n\overline{\alpha}_{j-1}^n\right)\end{bmatrix},$$

where $\overline{p}_{1,j+1/2}^n$ and $\overline{p}_{2,j+1/2}^n$ – dispersed phase and gaseous phase pressures from the solution of the Riemann problem.

One of the main advantages of the Godunov approach for the numerical flux through the computational cell edge calculation is the intrinsic coupling between the phases without artificial splitting strategies for the most challenging case when the dispersed phase volume fraction to the left of the edge significantly differs from that to the right. Another important feature is the possibility of correct treatment of the special cases when the dispersed phase on one side of the initial discontinuity vanishes. To satisfy the hyperbolicity conditions (3) the special cases demand very small but non-zero dispersed phase volume fraction in each cell of the computational area. So the modeling of the SW interaction with the particles cloud is possible. Note that in the areas where the gradient of the dispersed phase volume fraction is small the non-conservative term in (1) can be omitted and the equations for gaseous and dispersed phases decouple.

The system of ordinary differential equations for the inter-phase interaction terms is solved at the second stage of the numerical algorithm for the time step integration with the use of explicit Euler scheme.

Godunov method is verified on a series of Riemann problems [13] with the initial conditions which provide the main types of the flow that cause the difficulties in numerical modeling including the cases with huge, up to several orders variations in the parameters of phases and parameters to the left and to the right of the initial discontinuity. Consider as an example the following rough Riemann problem:

$$\overline{\alpha}_L=0.2,\ \overline{\rho}_L=1900,\ \overline{v}_L=0,\ \overline{p}_L=10,\ \rho_L=2,\ v_L=0,\ p_L=3,\ x<0.5,$$
$$\overline{\alpha}_R=0.9,\ \overline{\rho}_R=1950,\ \overline{v}_R=0,\ \overline{p}_R=1000,\ \rho_R=1,\ v_R=0,\ p_R=1,\ x>0.5,$$
$$\gamma=1.35,\ \overline{\gamma}=3,\ \overline{P}_0=3400.$$

Subscript “L” corresponds to the parameters to the left from the initial discontinuity, “R” – to the right. Computational grid is uniform with the cells number equal to 100. Fig. 1 illustrates predicted pressures and densities of the phases in comparison with the exact solutions. Time step is chosen dynamically to satisfy stability criteria, CFL number is equal to 0.8. The flow field includes “left” SW and “right” rarefaction wave for the dispersed phase and two shock waves for the gaseous phase.

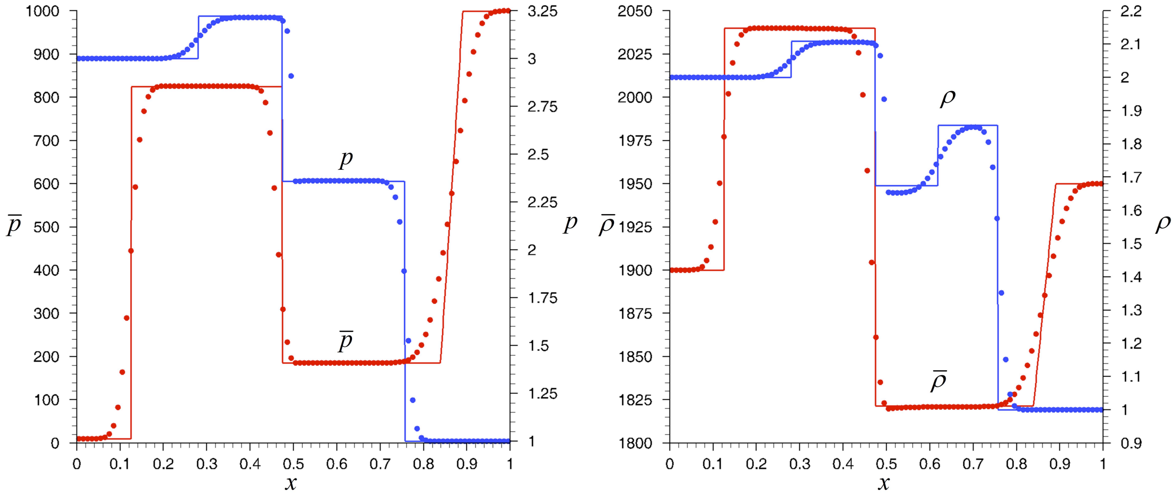

(a) (b)

Figure 1. Solution of the test Riemann problem: (a) profiles of pressures; (b) profiles of densities.

4 Statement of the problem

Statement of the problem corresponds to one of the experiments in [9]. The similar modeling was carried out in [5]. The part of the shock tube with the length L = 1.8 m filled with the air under normal conditions is considered (see Fig. 2). The non-penetrating and inflow conditions are imposed at the left and right boundaries respectively. The compression stage of the SW in the experiment allows to impose constant parameters at the right boundary corresponded to that behind the SW with Mach number 1.3 (p = 1.8 atm, v = 151 m/s, ρ = 1.82 kg/m^3) during the whole computational time 4 ms.

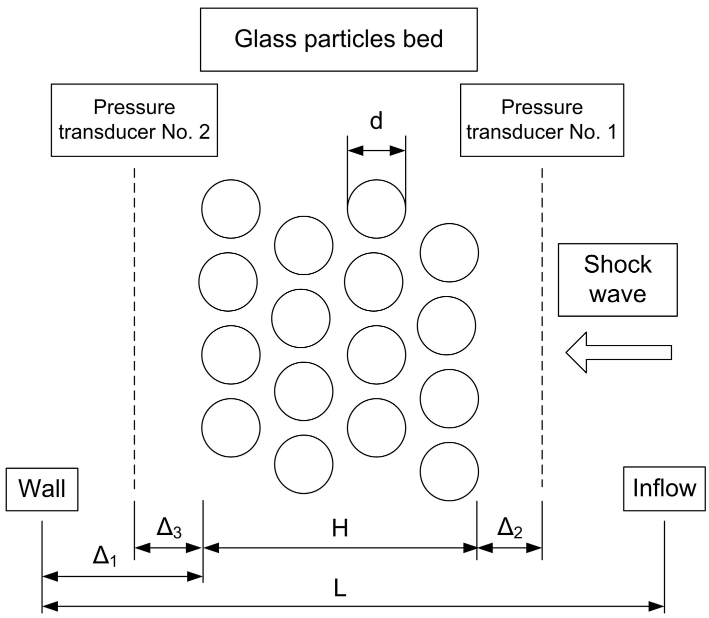

Figure 2. Schematic statement of the problem about SW – glass particles cloud interaction.

The left boundary of the glass particles cloud with the length H = 2 cm is located at the distance Δ_1 = 0.89 m from the left boundary of the computational area. The diameter of the particles d = 1.5 mm, initial dispersed phase volume fraction is equal to 0.65. The dispersed phase is considered to be

weakly compressed media with the initial density $\bar{\rho} = 2500\ \mathrm{kg/m^3}$, corresponded to the glass density, and the following parameters of the equation of state in (1): $\bar{\gamma} = 2.5$, $\bar{P}_0 = 10^3$ atm. The drag coefficient in (2) is taken equal to the constant value 0.6 in accordance to the recommendations in [9].
Gas pressure is measured in the experiment by means of two pressure transducers. The first one is located to the right of the particles bed at the distance Δ_2 = 0.11 m. The second one – at the distance Δ_3 = 0.043 m to the left of the bed.
The major goal of the problem consideration is to obtain the qualitatively and quantitatively correct wave structure which includes reflected wave (RW) and transmitted wave (TW) taking into account the motion of the particles cloud.

5 Results of modeling

Interaction of the incident SW with the dense particles cloud produces two waves – the RW which is seen at the transducer No. 1 at the time moment about 2.4 ms in Fig. 3a and the TW noticeable at the transducer No. 2, time moment about 2.2 ms. The correct calculated time gap between the moments of RW and TW arrivals to the transducers in comparison with the experimental one testifies to the adequate model of the drag force in use. The relative error in the amplitude for the RW is about 5% and for the TW is about 9%. Note the similar discrepancy and tends for pressure curves in the calculations in [9]. It needs to mention that the correct wave-pattern within the framework of the mathematical model in use is obtained due to the careful treatment of the non-conservative right-hand side terms in the BN equations on the basis of Godunov approach.
Another important feature of the experiment is the motion of the particles cloud. The motion is conditioned by the difference of the gas pressures at boundaries of the cloud as well as by the friction force action. Fig. 3b illustrates the predicted position of the cloud at the time moment 3.6 ms – the left boundary displaced at about 1 cm from its original position.

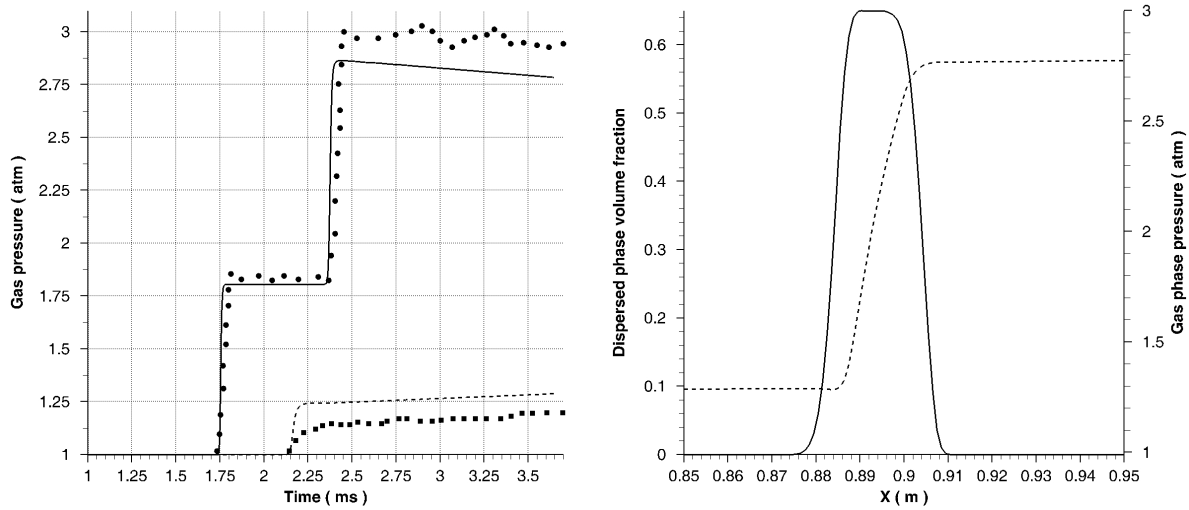

(a) (b)

Figure 3. Results of the modeling: (a) comparison of experimental (circles, transducer No. 1 and squares, transducer No. 2) and calculated (solid line, transducer No. 1 and dashed line, transducer No. 2) pressures at the transducers; (b) predicted distributions of dispersed phase volume fraction (solid line) and the gas phase pressure (dashed line) at the time moment 3.6 ms.

Conclusions

The mathematical modeling of shock wave interaction with dense particles cloud is carried out. The investigation is performed by means of specially developed one-dimensional computer code which

solves Baer-Nunziato equations with the use of Godunov method. Method realization is verified on a series of Riemann problems. The important feature of the Godunov approach is the possibility of correct treatment of the special cases when the dispersed phase on one side of the initial discontinuity vanishes.
The main features of the shock wave – particles cloud interaction process are obtained in the calculations including reflected and transmitted waves as well as the motion of the particles cloud. The calculated quantitative characteristics of the process – waves amplitudes and velocities – are in good agreement with the natural experiment.

Acknowledgements

This work is supported by the Russian Science Foundation under grant 14-50-00005 and performed in Steklov Mathematical Institute of Russian Academy of Sciences.

References

[1] Gidaspow D. (1994). Multiphase Flow and Fluidization. Academic Press. (ISBN 978-0-12-282470-8).

[2] Houim RW, Oran ES. (2014). A technique for computing dense granular compressible flows with shock waves. arXiv:1312.1290v2 [physics.comp-ph] 17 Oct 2014.

[3] Liu H, Guo Y, Lin W. (2014). Simulation of shock-powder interaction using kinetic theory of granular flow. Powder Tech. doi: 10.1016/j.powtec.2014.12.031.

[4] Baer MR, Nunziato JW. (1986). A two-phase mixture theory for the deflagration-to-detonation transition in reactive granular materials. Int. J. Multiph. Flow. 21(6): 861.

[5] Abgrall R, Saurel R. (2003). Discrete equations for physical and numerical compressible multiphase mixtures. J. Comp. Phys. 186: 361.

[6] Khmel' TA, Fedorov AV. (2014). Description of dynamic processes in two-phase colliding media with the use of molecular-kinetic approaches. Comb., Expl., Shock Waves. 50(2): 196.

[7] Regele JD, Rabinovitch J, Colonius T, Blanquart G. (2014). Unsteady effects in dense, high speed, particle laden flows. Int. J. Multiphase. Flow. 61: 1.

[8] Schwendeman DW, Wahle CW, Kapila AK. (2012). The Riemann problem and high-resolution Godunov method for a model of compressible two-phase flow. J. Comp. Phys. 212: 490.

[9] Rogue X, Rodriguez G, Haas JF, Saurel R. (1998). Experimental and numerical investigation of the shock-induced fluidization of a particles bed. Shock Waves. 8: 29.

[10] Knight JB, Fandrich CG, Lau CN, Jaeger HM, Nagel SR. (1995). Density relaxation in a vibrated granular material. Phys. Review E. 51(5): 3957.

[11] Toro EF. (2009). Riemann Solvers and Numerical Methods for Fluid Dynamics. Springer, 3rd ed. (ISBN 978-3-540-25202-3).

[12] Andrianov N, Warnecke G. (2004). The Riemann problem for the Baer-Nunziato two-phase flow model. J. Comp. Phys. 195: 434.

[13] Tokareva SA, Toro EF. (2010). HLLC-type Riemann solver for the Baer-Nunziato equations of compressible two-phase flow. J. Comp. Phys. 229: 3573.